Three filters intravital fluorescence microscopy evaluation of tissue loss progression induced by ligatures in experimental peri-implantitis in a dog model

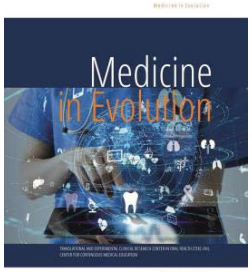

Rusu D.[1], Stratul S.I.[1], Boariu M.I.[2], Luchian I.[3], Boldeanu C.[1], Calniceanu H.[1], Vela O.[1], Kardaras G.[1], Chinnici S.[1], Veja I.[1], Igna V.[4], Roman A.[5], Soanca A.[5]

[1]Department of Periodontology, Faculty of Dental Medicine, Anton Sculean Research Center for Periodontal and Peri-Implant Diseases, "Victor Babes" University of Medicine and Pharmacy Timisoara
[2]Department of Endodontics, Faculty of Dental Medicine, TADERP Research Center, "Victor Babes" University of Medicine and Pharmacy Timisoara
[3]Department of Periodontology, Faculty of Dental Medicine, "Grigore T. Popa" University of Medicine and Pharmacy Iaşi
[4]University of Life Sciences „King Mihai I" of Timisoara, Faculty of veterinary Medicine, Department of Clinical Education Timisoara
[5]Department of Periodontology, Faculty of Dental Medicine, Applicative Periodontal Regeneration Research Unit, Iuliu Hatieganu University of Medicine and Pharmacy Cluj Napoca

Correspondence to:
Name: Ionut Luchian
Address: Department of Periodontology, Faculty of Dental Medicine, "Grigore T. Popa" University of Medicine and Pharmacy, 16 Universităţii Street, 700115 Iaşi, Romania
Phone: +40 745140641
E-mail address: ionut.luchian@umfiasi.ro

Abstract

Objectives: Tissue breakdown was obtained by placing ligatures around dental implants on the same edentulous dog hemimandible. Evaluation of hard tissue loss progression was performed using intravital fluorochrome labeling, as an alternative to standard light microscopy, on thin sections of non-demineralized hybrid bone-implant specimens. Material and Methods: Intravital fluorochrome labeling was administered by intraperitoneal injection of oxytetracycline and alizarin red S. Sections were cut, stained and evaluated by light microscopy and under the epifluorescent microscope. Bone loss architecture was analyzed under three filters: UV, green and red. Results: Epifluorescence microscopy demonstrated continuous bone activity in the surrounding area of the implants during the healing period. LM confirmed the intense cellular activity in the hard tissues around the implants. Conclusion: Within the limits of the present study, epifluorescence can be seen as a complementary approach to the LM "golden standard", providing both reliable and sufficient information with regard to bone resorption/apposition kinetics.

Keywords: animal study, dental implant, ligature induced, peri-implantitis, intravital fluorochrome labeling, light-microscopy, epifluorescence

INTRODUCTION

Extensive research into the peri-implantitis field has led to the conclusion that it is the most common biological complication in implant treatment [1-5]. Peri-implantitis is defined in the latest Classification for Periodontal and Peri-implant Diseases and Conditions (2018) as a plaque-associated pathologic condition occurring in the tissue surrounding dental implants, characterized by inflammation in the peri-implant mucosa and subsequent progressive loss of supporting bone [6]. While imagistic data during bone support loss in humans may be easily collected [7], additional histopathological data concerning peri-implant modifications can only be obtained through soft and hard tissue biopsies, which are governed by technical and ethical guidelines [8]. So far, the animal model, especially with regard to dogs, was thought to be a reliable source of details on tissue reactions in experimentally induced peri-implantitis [8-11].

The most frequently employed fluorescence microscopy method in life sciences is epifluorescence microscopy, also known as wide-field fluorescence microscopy (WFM). Fluorescence microscopy enables the detection of cell morphology, cellular/subcellular compartments, and disease or phenotypic indicators [12]. Fluorescence is described as the ability of some substances to transform short wavelengths of light into longer visible wavelength radiation [13]. The intrinsic ability of substances to fluoresce when exposed to an exciting UV light source is referred to as primary fluorescence (autofluorescence). The fluorescence created in substances by the application of fluorescent chemicals or dyes (fluorochromes) is known as secondary fluorescence [14, 15]. The administration of fluorochromes in animal models allows researchers to identify bone and cartilage development, remodeling dynamics and regeneration, which are critical criteria in bone tissue engineering investigations [16-18].

Fluorochromes have been used in bone research since the 1950s and are widely accepted substances. Several pioneers, for example Harold Frost, have carefully examined the possibilities of fluorochrome usage in bone formation and bone remodeling dynamics research, also in human studies, where he investigated several diseases [19-21]. Since the introduction of bone tissue engineering, there has been an increasing interest in the benefits of fluorochrome usage.

Fluorochrome labeling is based on the idea that some stains can bind directly to hydroxyapatite, the major component of bone, via calcium chelation. This occurs in all areas where new bone is formed [16, 20, 22]. Fluorochrome staining is highly effective for learning more about the beginning of the bone formation process (at the implant surface or another region of the implant) and bone remodeling activities surrounding implants. The mineralization process of newly produced bone may be entirely observed when the labels employ variation in fluorescent color and are supplied at different time-points. The labels can be administered to experimental animals subcutaneously, intraperitoneally, intramuscularly, or intravenously [16, 23].

Different intravital labeling protocols have been suggested in the processing of the bone specimens, some of which also contained dental implants. As indicators of new bone development, fluorochromes such as alizarin red S [24, 25]/complexone [26-28], calcein green [28, 29]/blue [27, 30], tetracycline [33-33] /oxytetracycline [16, 28, 34, 35], or xylenol orange [27, 35, 36] and more recently BAPTA labeling may be administered [27]. Tetracycline meets the characteristics of Frost's ideal bone label, as established in 1983. It represents the fluorochrome of choice in clinical studies, due to their non-toxic, cheap, easy to give, generally accessible, stable nature. Also, they present high affinity for calcium and are

incorporated at the site of active mineralization of hydroxyapatite and may be used as a tissue time-point marker [16, 23, 37-39].

Oxytetracycline can aid in determining the quantity of new bone development. It is exclusively visible in UV light, excites around 365-490 nm, emits at 520-570 nm, and fades fast. According to some authors [14, 23, 40, 41], it bounds to apatite and fluoresced yellow, yellowish-green, or leaf green; however, others claim that labelled new and old bone fluoresced bright golden yellow and dark sea green, respectively [42 43]. Continuous bone labeling allows for the assessment of total new bone formation and is often performed by administering the substance at doses that do not exceed 50 mg/kg to minimize adverse effects on osteogenesis [44].

Alizarin red S label provides strong contrast between cells, soft tissues, and calcified tissues. It excites at 530-580 nm and emits at 600-645 nm [16]. Green light is optimal for excitation of alizarin to fluoresced red light. At a dosage of 25-30 mg/kg, this chemical appears to be well tolerated in all species [14, 23, 28, 40, 45]. Because fluorochromes are bound in skeletal tissues as calcium complexes, proper histological processing is required. Optimum fluorochrome label preservation is attained when the fixed specimens are treated without interruption until they are embedded in plastic, and non-decalcified bone histology is performed before the microscopical examination [23]. It is also not required to utilize thicker sections for brighter fluorescence when using appropriate microscopic equipment, as opposed to thinner sections. However, multiple labels are more easily observed in thinner sections [23, 46, 47]. Additional filters are also useful in obtaining supplementary data, such as the red filter, that allows a label to be visible when it is excited at 510-560 nm and has the emission point of 573-648 nm [48]. In our study, this range covers both alizarin red S label and oxytetracycline.

Fluorescence microscopy is performed utilizing a microscope that has a fluorescence illuminator. Essentially, unstained sections are exposed to a light of a particular length (or wavelengths), which is absorbed by fluorophores and causes them to emit light of longer wavelengths (i.e., a different color than the absorbed light). A spectrum emission filter separates the transmitted light from the considerably weaker emitted fluorescence. In studies evaluating treatment strategies for peri-implantitis lesions, this method enhances the evaluation of both the direction and topographic localization of new bone growth [22, 40].

Multiple intravital fluorochrome labeling has been occasionally used for the study of bone formation following surgical intervention in the same animal over a certain period of time [49], and it is a common technnique to track the osseointegration of implants over time [50-52]. However, the literature does not mention studies using together green, red and UV filters to visualise intravital fluorochrome labeling to evaluate primarily the tissue loss around experimentally-induced peri-implantitis on non-decalcified sections. As data obtained under fluorochrome microscope are not influenced by the filter used, this method may be of interest in the study of lesions with hybrid consistency, like peri-implantitis.

Aim and objectives

The aim of this pilot study was to determine whether the tissue loss progression during experimental peri-implantitis in ligatured implants placed on the same edentulous dog hemimandible, using intravital fluorochrome labeling can be successfully observed using green, red and UV filters, as an alternative to standard light microscopy, on thin sections of non-demineralized hybrid bone-implant specimens.

MATERIAL AND METHODS

This pilot study was conducted in a single animal to reduce the number of experimental animals to be sacrificed, so that most of the information could be obtained.

The experiment was performed on one ten-years old adult half-breed dog, with a fully erupted permanent dentition (male, body weight 20 kg). The dog was housed under good conditions (in a single kennel with indoor and outdoor areas, room temperature range was approximately 18°C, with humidity above 30%) and fed once a day using granulated dog food and water *ad libitum*. Clinical examination determined that the dog was in good general health, with no systemic diseases [34].

Dental implants consisted of 5 titanium cylinders (3.3 mm, two 3.8 mm and two 4.1 mm in diameter, all 8 mm in length). All implants were fabricated by OT medical GmbH, Germany.

Operative procedures

All surgical procedures were carried out under general anesthesia (intravenous Diazepam 0,5%, 0,4mg/kg I.V. and Ketamine 10%, 10mg/kg I.V., endo-tracheal intubation 2–5% isoflurane gas). To maintain hydration, the animal received a constant-rate infusion of Ringer's solution while anesthetized. The protocol of the whole experiment was approved by the Ethical Commission of Scientific Research of UMFVBT (approval Nr. 06-16/09.01.2019). The timeline of the experiment is presented in Figure 1.

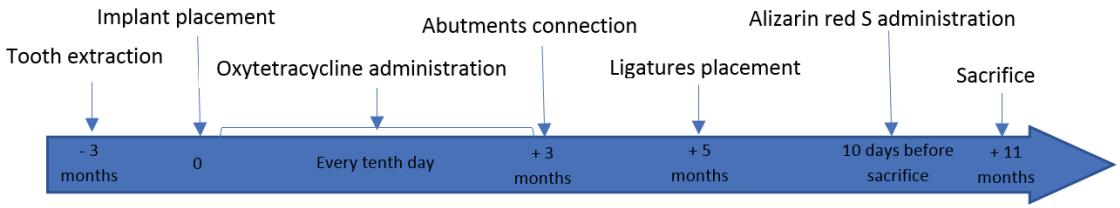

Figure 1. Timeline of the experiment

Postoperative procedures

Implants were exposed 3 months post-implantation and their healing abutments were connected (Figure 2). No oral hygiene regimen was administrated during this period, so that the peri-implant inflammation could initiate spontaneously. Five months post-implantation (two months post implant exposure), to accelerate the progression of the initial lesions, cotton ligatures were placed according to the method described by Lindhe et al. [53] in a submarginal position around the neck of implants. (Figure 3). The ligatures were not replaced or removed during this experiment. The animal was then fed a soft diet to induce plaque accumulation and to provoke peri-implant inflammation and bone resorption.

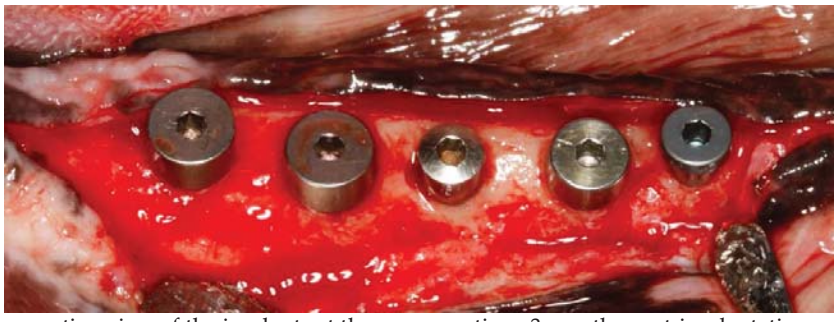

Figure 2. Intra-operative view of the implants at the exposure time, 3 months post-implantation, with the healing abutments in place. Note the integrity of the buccal and proximal bone

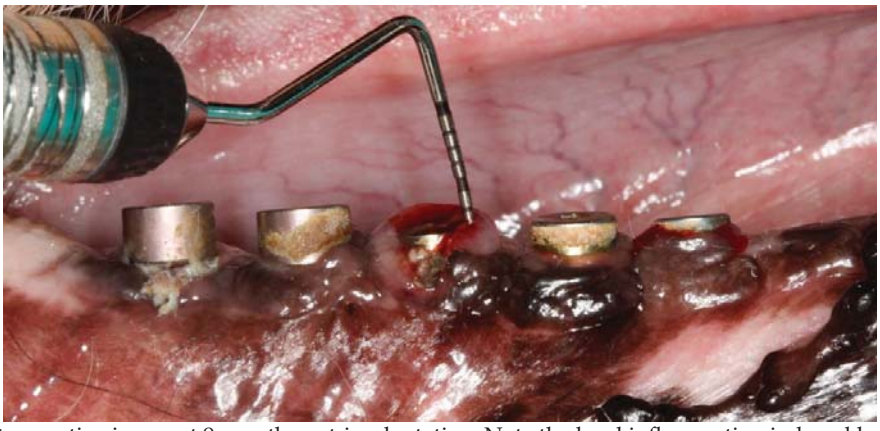

Figure 3. Post-operative image at 9-month post-implantation. Note the local inflammation induced by the ligatures

Intravital polyfluorochrome labeling was carried out for the histological evaluation of the bone reactions by intraperitoneal injection of oxytetracycline (OXY L.A. INJ, Dopharma BV, Raamsdonksveer, Holland), 50 mg/kg body weight, every tenth day, from implant placement until abutment installation for assessing the total new bone formation and alizarin red S 1% (Merck KGaA, Darmstadt, Germany), 40 mg/kg body weight, 10 days before sacrifice, to evidence bone remodeling around implants.

Histological preparation of the specimens

At the end of the experiment, 8 months after abutments were installed, the dog was sacrificed under general anesthesia (sodium pentobarbital: 200 mg/kg I.V.). The part of the jaw including the implants was sectioned and fixated in 10% neutral buffered formalin until laboratory processing.

The detailed histological protocol of the experiment was presented in a previously published paper (Boldeanu et al. 2022) [54]. In brief, Technovit 9100 (Kulzer GmbH, Hanau) embedding resin was used for the infiltration and embedding steps. Sections were prepared using the cutting/grinding method described by Donath & Breuner [55] on a cutting/grinding system (Exakt, Norderstedt, Germany). The polymerized resin blocks containing the embedded sample were trimmed and transferred to glass slides. A cut was performed in buccal-lingual direction through the middle of each implant, in the long axis. For each implant, one section was carried out distally from the initial mid-section, while another section was carried out mesially, both in the long axis, so that two relatively equal central sections of 30 microns resulted. One section of each implant sample was stained with MOVAT Pentachrome (after Verhöff) (Morphisto, Frankfurt am Main, Germany) (MOV). After the staining of the sections, deplastination of the thin-sections was performed by incubation in two baths of acetone and twice in methoxyethyl-acetate (MEA). Finally, the stained slides were dehydrated and cover-slipped with a mounting medium. These stained sections were used in another research (Boldeanu 2022) [54].

The slides were analyzed and photographed using an epifluorescence Olympus® EX51 microscope (Olympus, USA) fitted with Canon E600 digital camera at x 4, x 10, x 40 and x 100 magnification. Three filters were used to analyze the slides: green filter for the alizarin red S stain, UV filter for the oxytetracycline stain and red filter for both of the labels. The images obtained were recombined using and the program ImageJ/FIJI (https://fiji.sc/) and examined with Aperio ImageScope software (version 12.4.6.5003, Leica Biosystems GmbH, Nussloch, Germany). For comparison, the stained thin sections were also scanned using the microscope slide scanner Leica Aperio® AT2 (Leica Biosystems, Wetzlar, Germany), under the 40x objective, that resulted in LM scanned slides.

The sections containing the fluorochrome-labeled tissues were kept in appropriate storage conditions, protected from intense light during processing, and were stored in the dark.

Histomorphologic analysis

On the alveolar crest and periosteal surfaces, plaque development and gingival inflammation, junctional epithelium-to-implant contacts, active or previous bone resorption, active bone formation, and the presence of fluorochrome labels were evaluated.

RESULTS

During the experimental peri-implantitis, none of the 5 implants failed. All implants presented heavy plaque accumulation, inflammation and bleeding, while implant no. 3 exhibited suppuration.

Histological observations

Both oxytetracycline and alizarin red S labels were observed when examinating the sections under UV filter (for the oxytetracycline label), green filter (for the alizarin red S filter) and red filter (for both labels). Figure 4 presents both of the labels, under the three filters, under various magnfications for better observation of their signal, knowing that longer exposure time allows the short-lived autofluorescent signal to fade out. Due to the long period of time of administration the substance during the osseointegration phase of the implants, oxytetracycline was evident under the UV filter as a wide yellow blurry line that was frequently found extending into the marrow space of the surrounding bone tissue (Figure 4A). As opposite, under the green filter, alizarin red S label formed a narrow intense red line extending outside the bone marrow, towards the osteons (Figure 4B). Toghether, both filters seemed to fuse under the red filter, however they remain destinguishable due to their variation in intensity (Figure 4C, x 100 magnification, 20 μm measure bar).

Epifluorescence microscopy demonstrated that there was continuous bone activity in the surrounding area of the implants during the healing period, as evidenced by the presence of high levels of oxytetracycline in this location. Fluorochrome labeling indicated an uneven pattern around the neck of the implants, as well as in the periosteal and endosteal areas. Cavities of bone growth, bone resorption, and bone remodeling were found around the implants in both green and UV filters. The oxytetracycline label was most prominent in the apical part of the implant, below the area where the ligatures provoked plaque-accumulation and subsequent bone resorption, whereas more alizarin red S than oxytetracycline could be detected surrounding the coronal part of the implants (Figure 5B), as bright red lines that are heavily disrupted. This observation was more evident under the red filter (Figure 5C). The kinetic data on bone turnover was observed using oxytetracycline sequential labeling of bone. From the time the implants were inserted until the abutments was placed, the substance was administered every 10 days. However, where bone resorption was experimentally initiated, subsequently irregular interrupted endosteal surface with scattered oxytetracycline label was observed. This can be interpreted as evidence of bone remodeling following the induced peri-implantitis. Implants were observed in close contact with the bone, as seen in the light microscopy section (Figure 6A), and fluorochromes apeared in close proximity to the implants. Other observations revealed significantly stained oxytetracycline rims at the implant interfaces, particularly in the apical threads (Figure 6B), more visible than the alizarin red S label (Figure 6C). This is confirmed by examining the sections under the red filter (Figure 6D).

The fluorescently labeled bone areas surrounding the implants showed a trend for intense alizarin red S label in the surrounding coronal tissue. When all threads in the cortical

area were labeled, the surrounding bone exhibited considerably higher oxytetracycline concentration.

Comparison between fluorochrome filters and LM mirror sections

In brief, the processed specimens showed partial osseointegration due to the induced peri-implantitis and subsequent bone resorption, deep peri-implant sulcus with damaged epithelial lining and extensive infiltrated connective tissue (ICT) difusion into the bone marrow (mainly constituted of inflammatory cells: lymphocytes and plasma cells with scattered neutrophils) separated by hyperemic blood vessels and a network of sporadic collagen fibers) (Figure 5A). There was a "subjective correlation" between new bone area and fluorocrome incidence. In areas between the threads of the fluorescent labeled sections and in the mirror LM ones, the distribution of new bone and fluorochrome occurrence followed the same pattern (Figure 6).

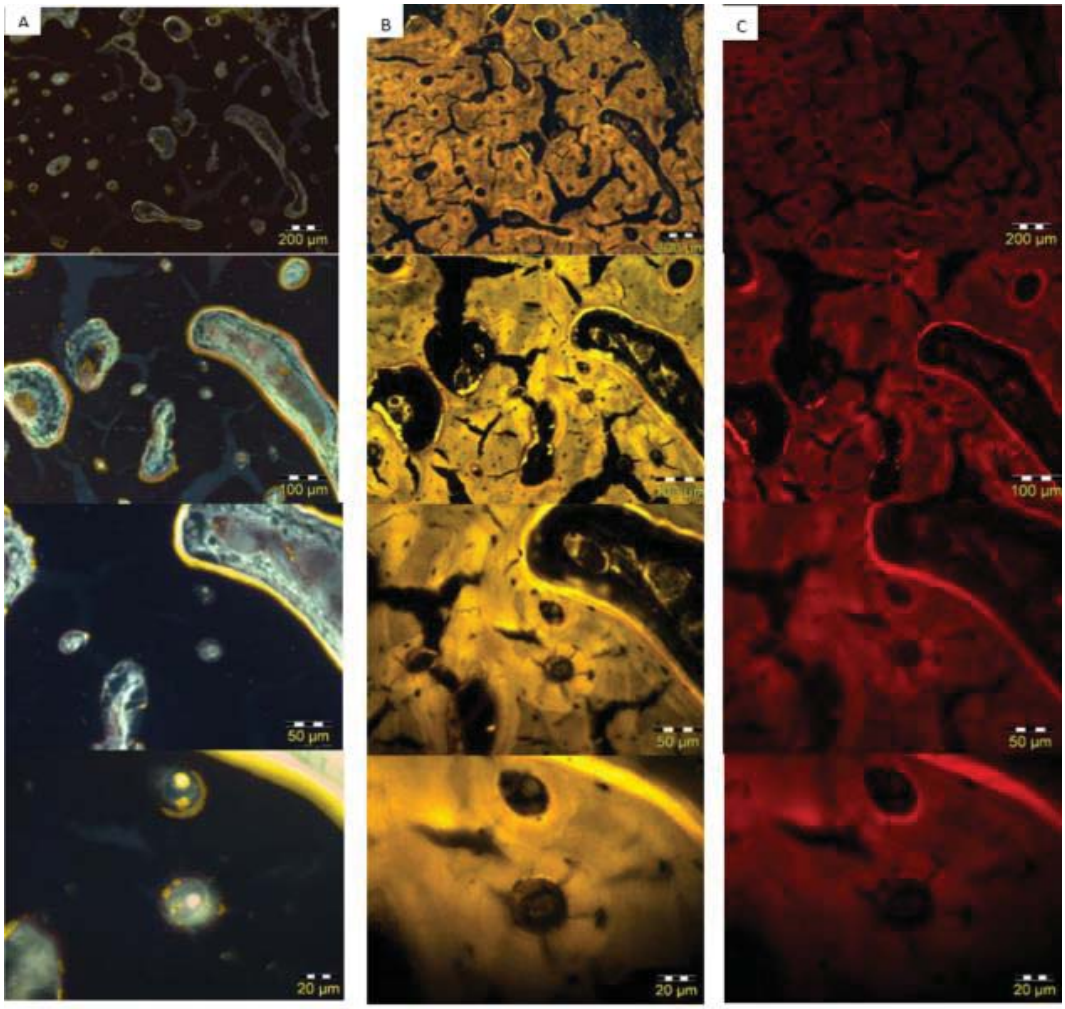

Figure 4. Detailed investigation of the surrounding hard tissues on the oral aspect of implant no. 3 under fluorochrome microscope UV filter (A), green filter (B) and red filter (C) (implant 3, scale on the images, x 4, x 10, x 40, x 100 magnification). Note the presence of the oxytetracycline lines deposited at the limit with the bone marrow under the UV filter (A, x 100 magnification). Alizarin red S is more evident at x 40 and x 100 magnification under the green filter, as a very narrow darker line towards an osteon (B, x 40). Under the red filter, both substances can be distinguished: oxytetracycline as a wide red blurry line and Alizarin red S as a narrow intense red line (C, x 100 magnification)

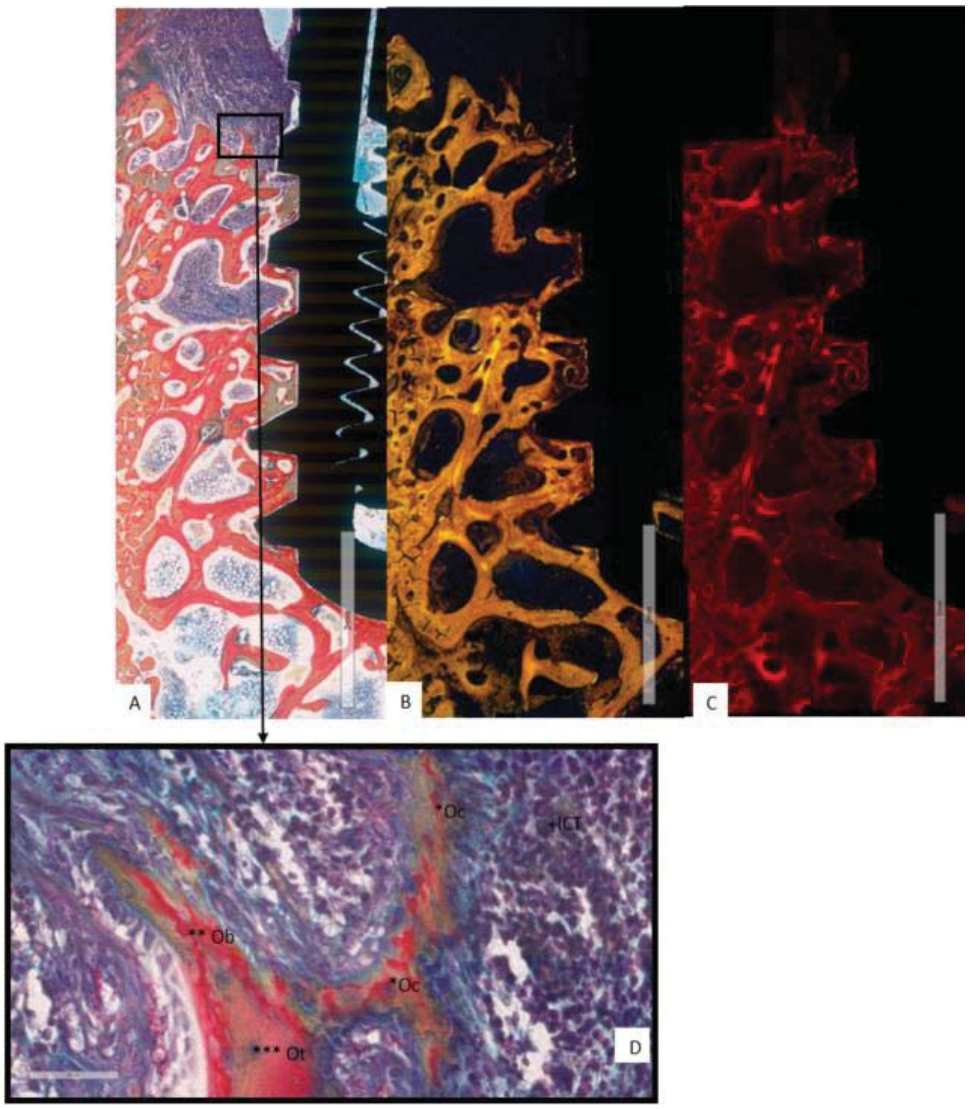

Figure 5. Scanned images of the implant and surrounding hard and soft tissue on the buccal aspect of implant no. 3. Observe the focal bone loss achieved by osteoclasts when activated by adjacent inflammation. Uneven endosteal surface is seen under light microscopy (A), fluorochrome microscope green filter (B), red filter (C) (implant 3, MOV staining, 2mm bar measure). In the detailed image (D), note the active alveolar bone remodeling involving giant multinucleated osteoclasts (*Oc), along with a osteoblast rim (**Ob) observed on the bone surface; osteocyte (***Ot) surrounding bone matrix is also observed along with a great amount of infiltrated connective tissue (+ICT) (LM image, bar measure 60 μm).

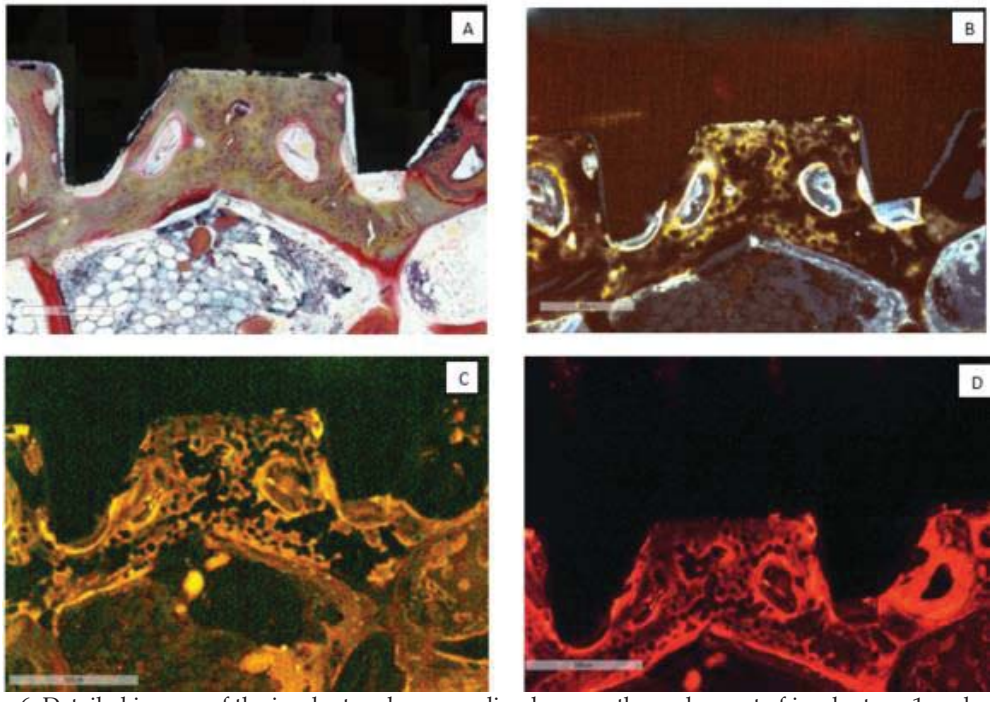

Figure 6. Detailed images of the implant and surrounding bone on the oral aspect of implant no. 1 under light microscopy (A), fluorochrome microscope UV filter (B), green filter (C), and red filter (D). Note the close contact between the bone and the implant, the new bone formation around the implants apically from the ligatures and the absence of histological signs of inflammation. Merging under the red filter, the two fluorochromes reveal that there was continuous bone activity in the vicinity of the implants during the healing period (D) (implant 1, MOV staining, x 4 magnification, bar measure 300µm)

DISCUSSIONS

In the present study we have explored the utilization of epi-fluorescence under three filters to observe the bone remodeling that occurs in an experimentally induced peri-implantitis. Bone labeling and microscope analysis appeared to be governed by the authors' unique selections, based on specific study aims, the quality of previous results and personal preferences, rather than a clear association between the label and the desired histological findings, as some authors have also noticed [16]. In general, the researchers give no explanation for selecting a specific intravital fluorochrome. Furthermore, there is a limited amount of histological literature comparing multiple intravital labels observed under varying filters.

In the majority of previous studies, the most commonly utilized approach for studying bone loss progression after experimentally induced peri-implantitis is light microscopy. Although conventional histology has shown to be a reliable method of evaluating the ossoeintegration of a dental implant, it is expensive, time consuming, damaging, and restricted to one or a few sections [56]. In comparison, epi-fluorescence allows the visualisation of the modifications of the bone architecture and the bone formation in time, by demarking the mineralization front at the time of administration without any further staining [16].

Utilizing fluorochrome labeling methods for *in vivo* bone research is not a novel development. Hunter documented alizarin, a madder dye, in bone remodeling research as early as the 1770s [57]. It shares calcium chelating and fluorescence capabilities with oxytetracycline, discovered in 1950 [58], and many other fluorochromes [16].

Only the emitted fluorescent light is permitted to pass through to the eye-piece or detector by using the appropriate light filters and mirror. Although in our study, both labels emitted in red color and the differences between them were small, each of them exhibited a characteristic fluorescence spectrum. This observation has also been noted by Pautke et al. when they experimented injecting 8 different substances into experimental models to assess the feasibility of sequential *in vivo* bone labeling using distinguishable fluorchromes [39].

Using multiple fluorochrome labeling and particular filter combinations offers many applications in experimental bone biology. In our study, we have used the UV filter to observe the oxytetracycline label (excited around 365-490 nm, and emitting at 520-570 nm), green filter for the alizarin red S label (excited at 530-580 nm and emitting at 600-645 nm) and red filter for both of them (for labels that were excited at 510-560 nm and with the emission point of 573-648 nm [48]. Rahn et al, have also applied a method that used intravital fluorochrome labeling of two substances and a special filter combination for allowing data gathering by computer-compatible systems, that resulted in improved image contrast in the fluorescence microscope [59].

While experimentally injected fluorescent substances are commonly used for the study of hard tissue mineralization and bone aposition/regeneration, fluorescence seems useful also for the study of bone resorptive processes, like in the present study of experimentally induced peri-implantitis. In addition to the informations obtained by conventional histology, in our study fluorescence has reflected the kinetics on bone turnover, with marked uneven endosteal surface and dispersed fluorochromic labels at the coronal part of the implants and with intense fluorochromic activity at the apical part of the implants. This is evidence of bone remodeling following the induced peri-implantitis in the coronal part and of osseointegration in the apical region of the implants. Similar observations have been noted by Carlsson et al. when investigating implant integration in both nondecalcified rutinely stained and fluorochrome labeled sections to determine if there was a resemblance between the methods. Analyzing the very same samples, like in our case, they have also noted that fluorescence microscopy can provide pertinent data as a complementary analysis [28]. With regard to mapping bone destructive processes, Weinlaender et al. initiated a radiation therapy to observe how the bone healing is influenced around three types of endoosseous dental implants in dogs. Similar to our observations, they had subjective estimations of parameters, though not yielding exact measurements like computer-assisted histomorphometric data, rendering supplimentary data about new bone formation and remodeing dynamics at different time intervals before and after onset of the radiation therapy, in their case, of the induced peri-implantitis, in our case [61].

Regarding the intravital fluorochrome administration sequence, with regard to oxytetracycline being administered after the implant placement and alizarin red S label few days before sacrifice, Marcaccini et al. obtained great results in determining when mineralisation occurs. In their study, the markers demonstrated different colors and provided sequential data, and their contrast made is possible to evaluate the changes during the experimental period. Similar observations are present also in our study, when observing where bone resorption was initiated, and generating subsequently uneven endosteal surface with scattered oxytetracycline label was observed.

After induction of peri-implantitis, clinical signs of inflammation were obviously more pronounced in the vicinity of the ligatures. These findings agreed well with the histological findings (Figure 5A) where a deep peri-implant sulcus with damaged epithelial lining and profound ICT infiltration of bone marrow was found. The onset of these changes around the ligatured implants can be evoked by analyzing the fluorescentely labelled sections, where the oxytetracycline infiltrated hard tissue has been lost. The remaining hard tissues appear to be uneven with scattered signs of label (Figure 5B). These finding were similar to those of

Zechner et al. [34], when the authors have investigated two types of implants, subjected to experimental peri-implantitis in dogs. In their study, various resorption of old and new peri-implant alveolar bone was present, and losses of alveolar bone-to-implant contact levels were seen. This applies also to our findings (Figure 5C).

CONCLUSIONS

Within the limits of this investigation, it can be concluded that properly fluorescence-labeled and processed sections of non-demineralized hybrid specimens of experimentally induced peri-implantitis in the dog model deliver quickly accessible additional information regarding the bone resorption mechanism. When compared to light microscopy, they can be analyzed promptly under an epi-fluorescence microscope to reveal significant data regarding bone remodeling. While conventional light microscopy is the "gold standard" in evaluating soft and hard tissues around dental implants, providing both reliable and sufficient information, fluorescence microscopy is a complementary approach, allowing for the measurement of bone activity around dental implants in both time and space, from the insertion point until the complete integration of the implants, and later, until complete tissue loss during peri-implantitis progression. Future studies may focus on refining and simplifying the examination protocol of the labeled hybrid specimens.

REFERENCES

1. Albouy, J.-P.; Abrahamsson, I.; Persson, L.G.; Berglundh, T. Spontaneous progression of peri-implantitis at different types of implants. An experimental study in dogs. I: Clinical and radiographic observations. Clin. Oral Implant. Res. 2008, 19, 997–1002.
2. Berglundh, T.; Persson, L.; Klinge, B. A systematic review of the incidence of biological and technical complications in implant dentistry reported in prospective longitudinal studies of at least 5 years. J. Clin. Periodontol. 2002, 29 (Suppl. S3), 197–212, discussion 232–233.
3. Fransson, C.; Lekholm, U.; Jemt, T.; Berglundh, T. Prevalence of subjects with progressive bone loss at implants. Clin. Oral Implant. Res. 2005, 16, 440–446.
4. Fransson, C.; Wennström, J.; Berglundh, T. Clinical characteristics at implants with a history of progressive bone loss. Clin. Oral Implant. Res. 2008, 19, 142–147.
5. Roos-Jansåker, A.M.; Lindahl, C.; Renvert, H.; Renvert, S. Nine- to fourteen-year follow-up of implant treatment. Part II: Presence of peri-implant lesions. J. Clin. Periodontol. 2006, 33, 290–295.
6. Schwarz, F.; Derks, J.; Monje, A.; Wang, H.L. Peri-implantitis. J. Periodontol. 2018, 89 (Suppl. S1), S267–S290.
7. Weiss, R., II; Read-Fuller, A. Cone Beam Computed Tomography in Oral and Maxillofacial Surgery: An Evidence-Based Review. Dent. J. 2019, 7, 52.
8. Albouy, J.-P.; Abrahamsson, I.; Persson, L.G.; Berglundh, T. Spontaneous progression of ligatured induced peri-implantitis at implants with different surface characteristics. An experimental study in dogs II: Histological observations. Clin. Oral Implant.Res. 2009, 20, 366–371.
9. Carcuac, O.; Abrahamsson, I.; Charalampakis, G.; Berglundh, T. The effect of the local use of chlorhexidine in surgical treatment of experimental peri-implantitis in dogs. J. Clin. Periodontol. 2015, 42, 196–203.
10. Ericsson, I.; Lindhe, J.; Rylander, H.; Okamoto, H. Experimental periodontal breakdown in the dog. Eur. J. Oral Sci. 1975, 83, 189–192.
11. Marinello, C.; Berglundh, T.; Ericsson, I.; Klinge, B.; Glantz, P.; Lindhe, J. Resolution of ligature-induced peri-implantitis lesions in the dog. J. Clin. Periodontol. 1995, 22, 475–479.

12. Liu, E., Vega, S., Dhaliwal, A., Treiser, M. D., Sung, H.-J., & Moghe, P. V. (2017). 3.19 High Resolution Fluorescence Imaging of Cell–Biomaterial Interactions ☆. Comprehensive Biomaterials II, 406–423.
13. Boyne PJ, Kruger GO. Fluorescence microscopy of alveolar bone repair. Oral Surg Oral Med Oral Pathol 1962;15:265–281.
14. Marcaccini AM, Novaes AB Jr, Souza SL, Taba M Jr, Grisi MF. Immediate placement of implants into periodontally infected sites in dogs. Part 2: A fluorescence microscopy study. Int J Oral Maxillofac Implants. 2003 Nov-Dec;18(6):812-9.
15. Capasso, L.; D'Anastasio, R.; Guarnieri, S.; Viciano, J.; Mariggiò, M. Bone natural autofluorescence and confocal laser scanning microscopy: Preliminary results of a novel useful tool to distinguish between forensic and ancient human skeletal remains. Forensic Sci. Int. 2017, 272, 87–96.
16. van Gaalen SM, Kruyt MC, Geuze RE, de Bruijn JD, Alblas J, Dhert WJ. Use of fluorochrome labels in in vivo bone tissue engineering research. Tissue Eng Part B Rev. 2010 Apr;16(2):209-17.
17. Bruneel B, Witten PE. Power and challenges of using zebrafish as a model for skeletal tissue imaging. Connect Tissue Res. 2015;56(2):161–73.
18. Chavassieux P, Chapurlat R. Interest of Bone Histomorphometry in Bone Pathophysiology Investigation: Foundation, Present, and Future. Front Endocrinol (Lausanne). 2022 Jul 28;13:907914.
19. Frost HM: Relation between bone tissue and cell population dynamics, histology and tetracycline labeling. Clin Orthop49:65–75, 1966.
20. Frost HM: Tetracycline-based histological analysis of bone remodeling. Calcif Tissue Res 3:211–237, 1969
21. Villanueva AR, Ilnicki L, Duncan H, et al: Bone and cell dynamics in the osteoporoses: a review of measurements by tetracycline bone labeling. Clin Orthop 49:135–150, 1966
22. Schwarz, Frank, Marfin Sager, and Jürgen Becker. "Peri-implantitis defect model." Osteology guidelines for oral and maxillofacial regenerations. Preclinical models for translational research, Quintessence (2011): 1-56.
23. An YH, Martin Kl. Handbook of histology methods for bone and cartilage. New Jersey, USA: Humana Press Inc; 2003.
24. Harris WH, Travis DF, Friberg U, et al. The in vivo inhibition of bone formation by alizarin red S. J Bone Joint Surg [Am] 1964;46:493–508.
25. Adkins KF. Alizarin red S as an intravital fluorochrome in mineralizing tissues. Stain Technol 1965;40:69–70.
26. Rahn BA, Perren SM. Alizarin complexone–fluorochrome for bone and dentine labeling. Experientia 1972;28:180
27. Pautke C, Vogt S, Tischer T, Wexel G, Deppe H, Milz S, et al. Polychrome labeling of bone with seven different fluorochromes: enhancing fluorochrome discrimination by spectral image analysis. Bone 2005;37:441–5.
28. Carlsson, C.; Holmgren-Peterson, K.; Jönsson, J.; Johansson, P.; Albrektsson, A.; Hoffman, M.; Sul, Y.-T.; Johansson, C.B. Comparing light- and fluorescence microscopic data: A pilot study of titanium- and magnesium oxide implant integration in rabbit bone. Online. TITANIUM Int. Sci. J. Dent. Implant. Biomater. 2009, 1, 61–70
29. Diehl H, Ellingboe JL. Indicator for titration of calcium in presence of magnesium using disodium dihydrogen ethylenediamine tetraacetate. Analytic Chem 1956;28:882–884.
30. Rahn BA, Perren SM. Calcein blue as a fluorescent label in bone. Experientia 1970;26:519–520.
31. Milch RA, Rall DP, Tobie JE. Bone localization of the tetracyclines. J Natl Cancer Inst 1957;19:87–93.
32. Milch RA, Rall DP, Tobie JE. Fluorescence of tetracycline antibiotics in bone. J Bone Joint Surg [Am] 1958;40:897–910.
33. Harris WH. A microscopic method of determining rates of bone growth. Nature 1960;188:1038–1039.
34. Zechner, W.; Kneissel, M.; Kim, S.; Ulm, C.; Watzek, G.; Plenk, H., Jr. Histomorphometrical and clinical comparison of submerged and nonsubmerged implants subjected to experimental peri-implantitis in dogs. Clin. Oral Implant. Res. 2004, 15, 23–33.

35. Park, S.-Y.; Kim, K.-H.; Rhee, S.-H.; Lee, J.-C.; Shin, S.-Y.; Lee, Y.-M.; Seol, Y.-J. An immediate peri-implantitis induction model to study regenerative peri-implantitis treatments. Clin. Oral Implant. Res. 2017, 28, 36–42.
36. Rahn BA, Perren SM. Xylenol orange, a fluorochrome useful in polychrome sequential labeling of calcifying tissues. Stain Technol 1971;46:125–129.
37. Frost HM (1963) Measurement of human bone formation by means of tetracycline labelling.Can J Biochem Physiol 41, 31–42.
38. Rahn B (1976) Die polychrome Sequenzmarkierung Intravitale Zeitmarkierung zur tierexperimentellen Analyse der Knochenund Dentinbildung. Freiburg: Habilitationsschrift.
39. Pautke C, Vogt S, Kreutzer K, Haczek C, Wexel G, Kolk A, Imhoff AB, Zitzelsberger H, Milz S, Tischer T. Characterization of eight different tetracyclines: advances in fluorescence bone labeling. J Anat. 2010 Jul;217(1):76-82.
40. Plenk, H., Jr. The microscopic evaluation of hard tissue implants. In Techniques of Biocompatibility Testing; Williams, D.F., Ed.; CRC: Boca Raton, FL, USA, 1986; Volume 1, pp. 35–81.
41. O'Brien FJ, Taylor D, Lee TC. An improved labelling technique for monitoring microcrack growth in compact bone. J Biomech 2002; 35:523 – 6
42. Frost HM. Preparation of undecalcified bone sections by rapid manual method. Stain Technol 1958;33:273–7.
43. Samit K. Nandi, Subhasish Biswas, Chapter 6 - In Vivo Characterization of Biomaterials, Characterization of Biomaterials, Academic Press, 2013, Pages 255-297, ISBN 9780124158009.
44. Frost HM: Bone histomorphometry: Choice of marking agent and labeling schedule. In: Recker RR, ed:Bone Histomorphometry: Techniques and Interpretation.CRC Press, Inc., Boca Raton,FL, 1983:37–52.
45. Miani A, Malossini L, Miani C: Alternate use of tetracycline and alizarin red S in the temporal study of osseous deposition. Boll Soc Ital Biol Sper40:1260–1262, 1964.
46. Birkenhager-Frenkel DH, Birkenhager JC: Bone appositional rate and percentage of doubly and singly labeled surfaces: comparison of data from 5- and 20-micron sections. Bone8:7–12, 1987.
47. Martin RB: Label escape theory revisited: the effects of resting periods and section thickness. Bone10:255–264, 1989.
48. Weber GF, Menko AS. Color image acquisition using a monochrome camera and standard fluorescence filter cubes. Biotechniques. 2005 Jan;38(1):52, 54, 56.
49. Erben RG, Scutt AM, Miao DS, et al: Short-term treatment of rats with high dose 1,25-dihydroxyvitamin D3stimulates bone formation and increases the number of osteoblast precursor cells in bone marrow. Endocrinology138:4629–4635, 1997
50. Jinno T, Goldberg VM, Davy D, et al: Osseointegration of surface-blasted implants made of titanium alloy and cobalt-chromium alloy in a rabbit intramedullary model. J Biomed Mater Res42:20–29, 1998
51. Schliephake H, Neukam FW, Hutmacher D, et al:Experimental transplantation of hydroxylapatite-bone composite grafts. J Oral Maxillofac Surg53:46–51, 1995.
52. Tisdel CL, Goldberg VM, Parr JA, et al: The influence of a hydroxyapatite and tricalciumphosphate coating on bone growth into titanium fiber-metal implants. J Bone Joint Surg [Am] 76:159–171, 1994.
53. Lindhe, J.; Berglundh, T.; Ericsson, I.; Liljenberg, B.; Marinello, C. Experimental breakdown of peri-implant and periodontal tissues. A study in the beagle dog. Clin. Oral Implant. Res. 1992, 3, 9–16.
54. Boldeanu, L.-C.; Boariu, M.; Rusu, D.; Vaduva, A.; Roman, A.; Surlin, P.; Martu, I.; Dragoi, R.; Popa-Wagner, A.; Stratul, S.-I. Histomorphometrical and CBCT Evaluation of Tissue Loss Progression Induced by Consecutive, Alternate Ligatures in Experimental Peri-Implantitis in a Dog Model: A Pilot Study. J. Clin. Med. 2022, 11, 6188.
55. Donath, K.; Breuner, G. A method for the study of undecalcified bones and teeth with attached soft tissues. The Säge-Schliff (sawing and grinding) technique. J. Oral Pathol. 1982, 11, 318–326.
56. Vandeweghe S, Coelho PG, Vanhove C, Wennerberg A, Jimbo R. Utilizing micro-computed tomography to evaluate bone structure surrounding dental implants: a comparison with histomorphometry. J Biomed Mater Res B Appl Biomater. 2013 Oct;101(7):1259-66.

57. Hunter, J. Treatise on the Natural History and Diseases of the Human Teeth. With Notes by Thomas Bell. London:Longman, Reese, Orme, Brown, Green and Norman, Paternoster-row, 1835.
58. Linsell, W.D., and Fletcher, A.P. Laboratory and clinical experience with terramycin hydrochloride. Br Med J2,1190, 1950.
59. Rahn BV, Bacellar FC, Trapp L, Perren SM. [A method for morphometry of bone formation using fluorochromes (author's transl)]. Aktuelle Traumatologie. 1980 Apr;10(2):109-115.
60. Park, S.-Y.; Kim, K.-H.; Rhee, S.-H.; Lee, J.-C.; Shin, S.-Y.; Lee, Y.-M.; Seol, Y.-J. An immediate peri-implantitis induction model to study regenerative peri-implantitis treatments. Clin. Oral Implant. Res. 2017, 28, 36–42.
61. Weinlander, M. Beumer,J., Kenney, B. Lekovic, V., Holmes, R., Moy, P., Plenk, H.: Histomorphometric and fluorescence microscopic evaluation of interfacial bone healing around 3 different dental implants before and after radiation therapy. Int. J. Oral and Maxillofac Implants. 2006. 21:212-224.